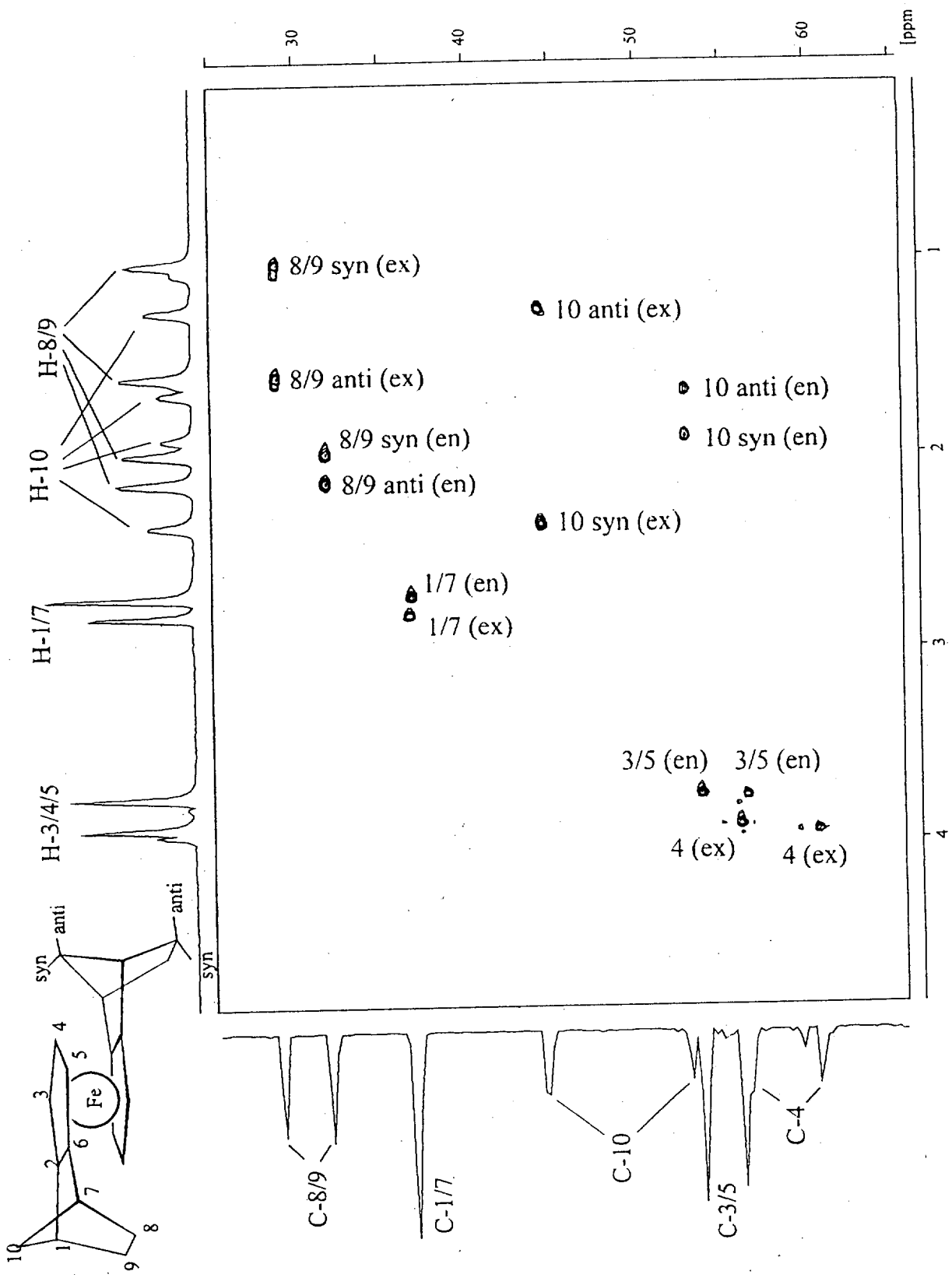

Figure S1. HMQC NMR spectrum of **3b** (600.14 MHz, C_6D_6, 300 K). (ex) and (en) = *exo*- and *endo*-bound ligand, respectively.

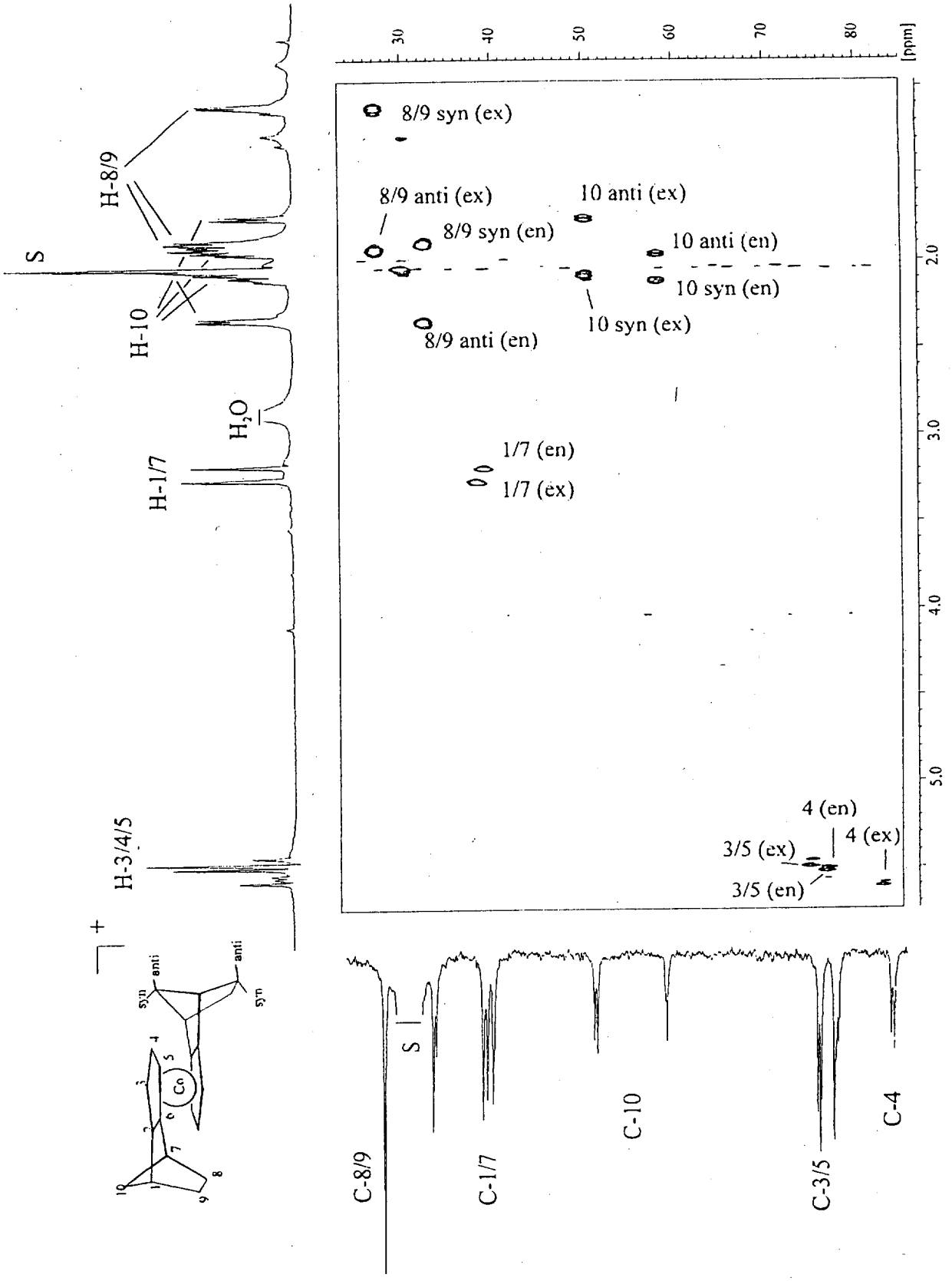

Figure S2. HMQC NMR spectrum of **6a**$^+$ PF_6^- (600.14 MHz, acetone-d_6, 300 K). S = solvent, (ex) and (en) = *exo*- and *endo*-bound ligand, respectively.

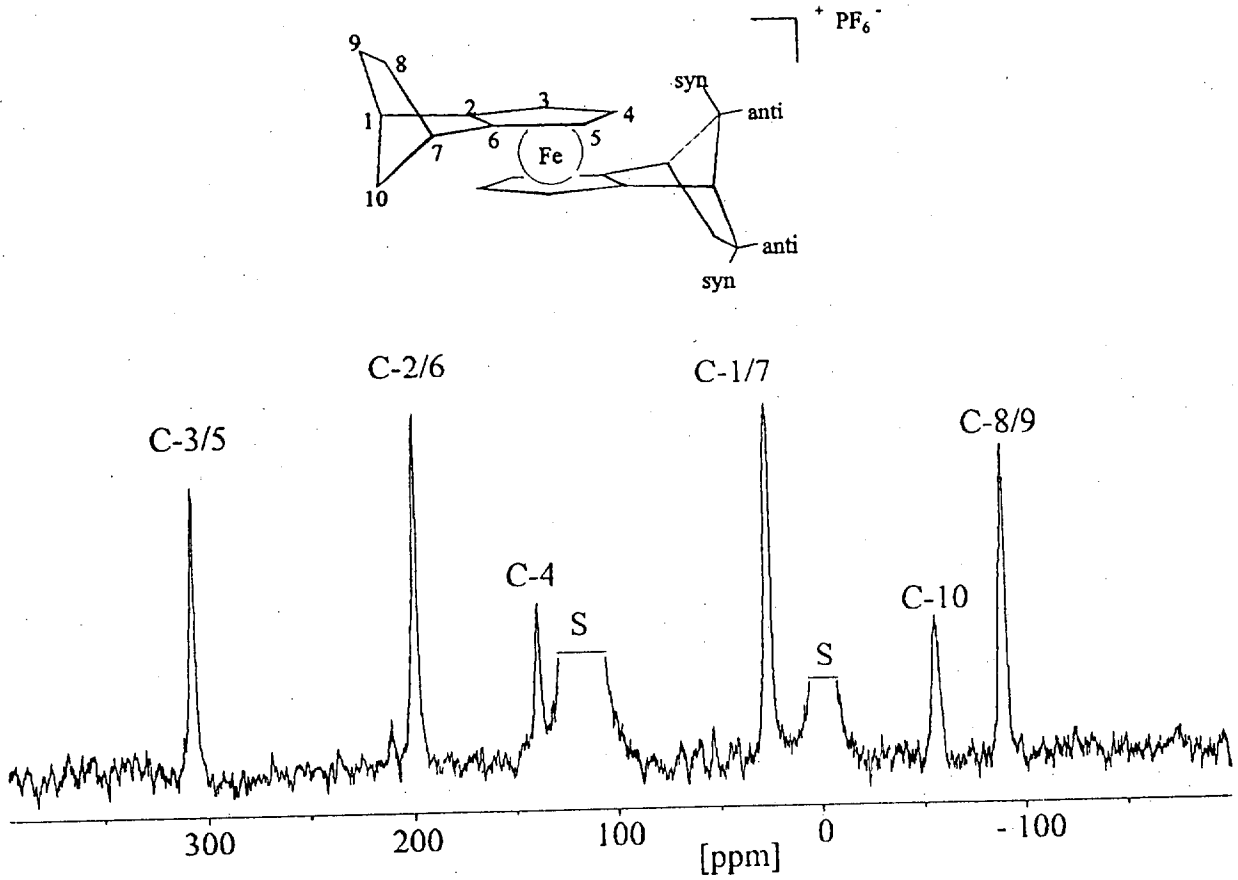

Figure S3. ^{13}C NMR spectrum of $\mathbf{3a}^{+}PF_6^{-}$ in CD_3CN at 305 K. S = solvent.

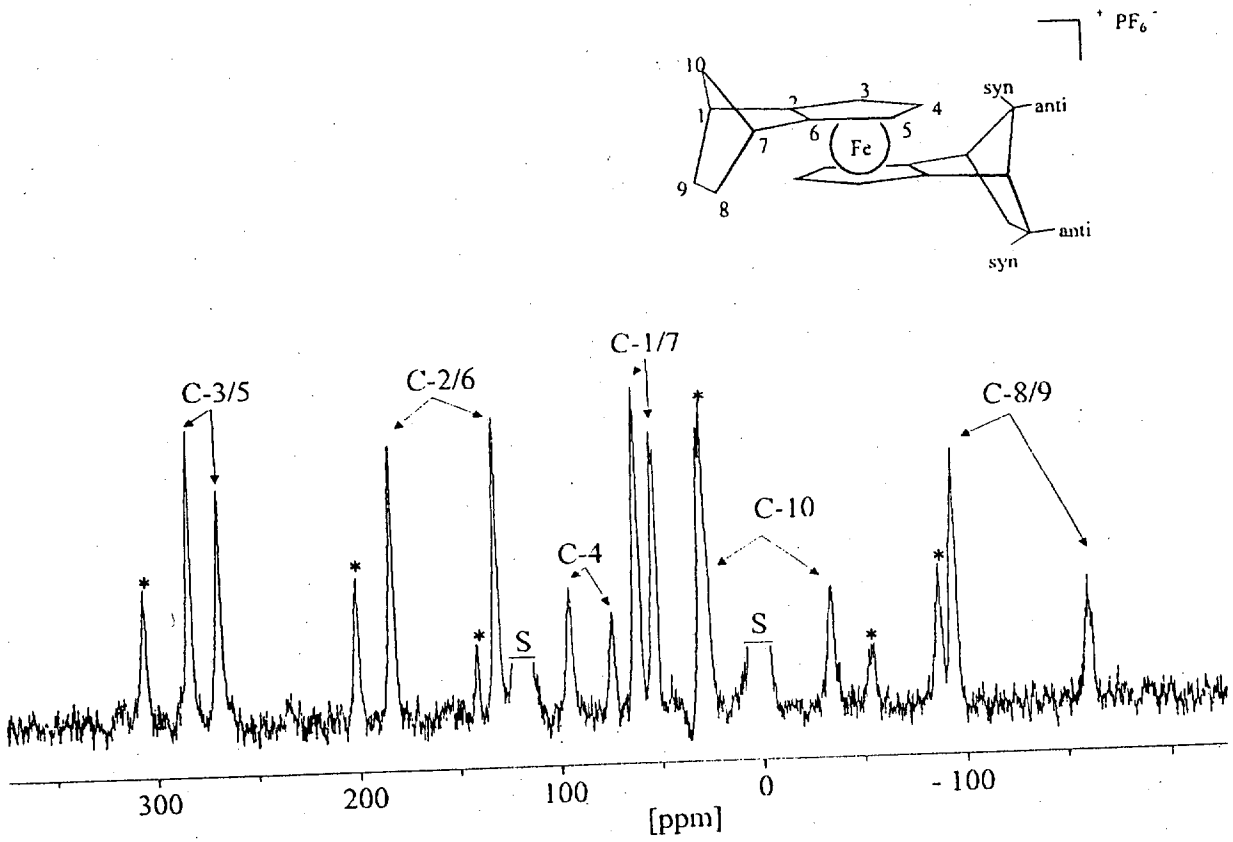

Figure S4: ^{13}C NMR spectrum of $\mathbf{3b}^{+}PF_6^{-}$ in CD_3CN at 305 K contaminated with $\mathbf{3a}^{+}PF_6^{-}$ (starred signals). S = solvent.

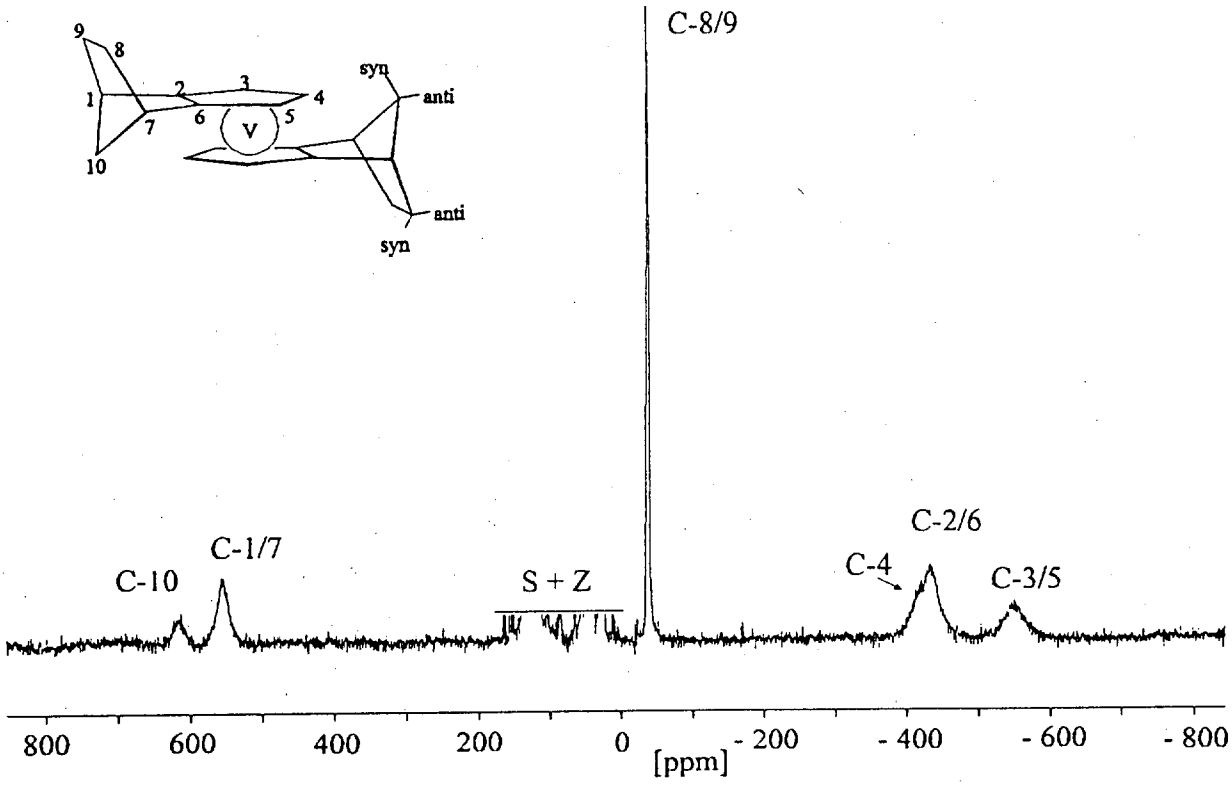

Figure S5. ^{13}C NMR spectrum of **4a** in toluene-d_8 at 345 K. S = solvent, Z = diamagnetic impurities.

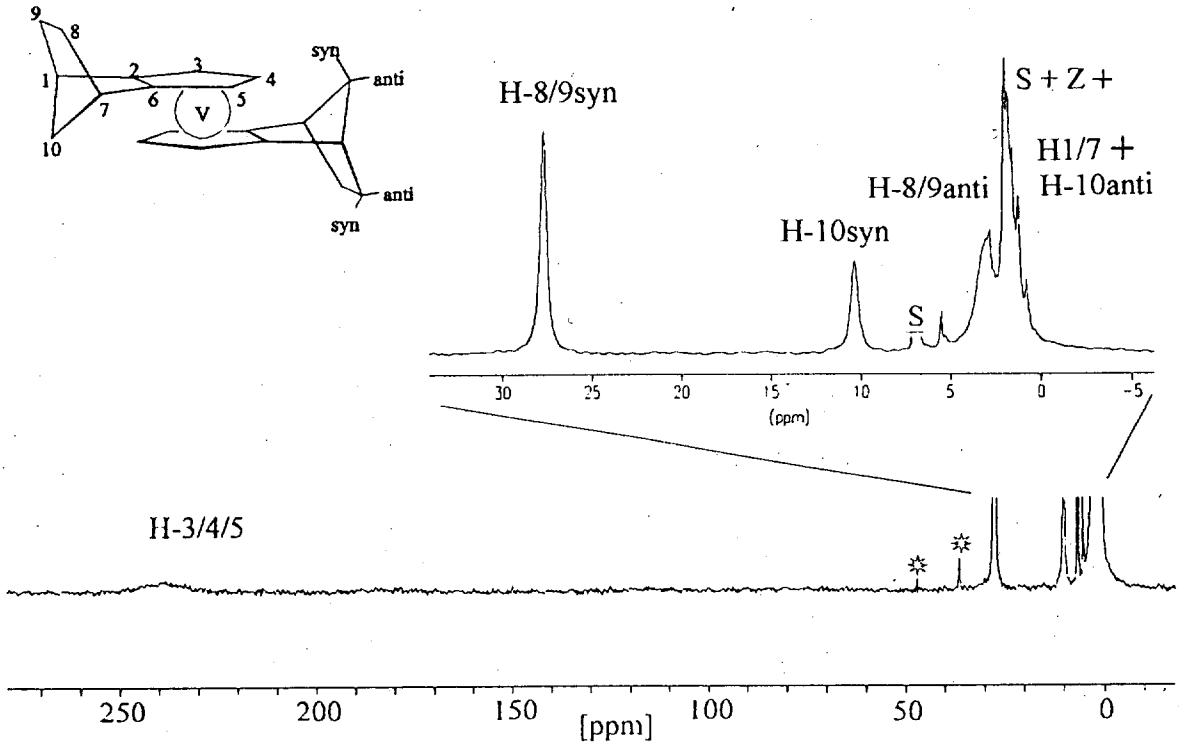

Figure S6. ^{1}H NMR spectrum of **4a** in toluene-d_8 at 345 K. S = solvent, Z and * = dia- and paramagnetic impurities, respectively.

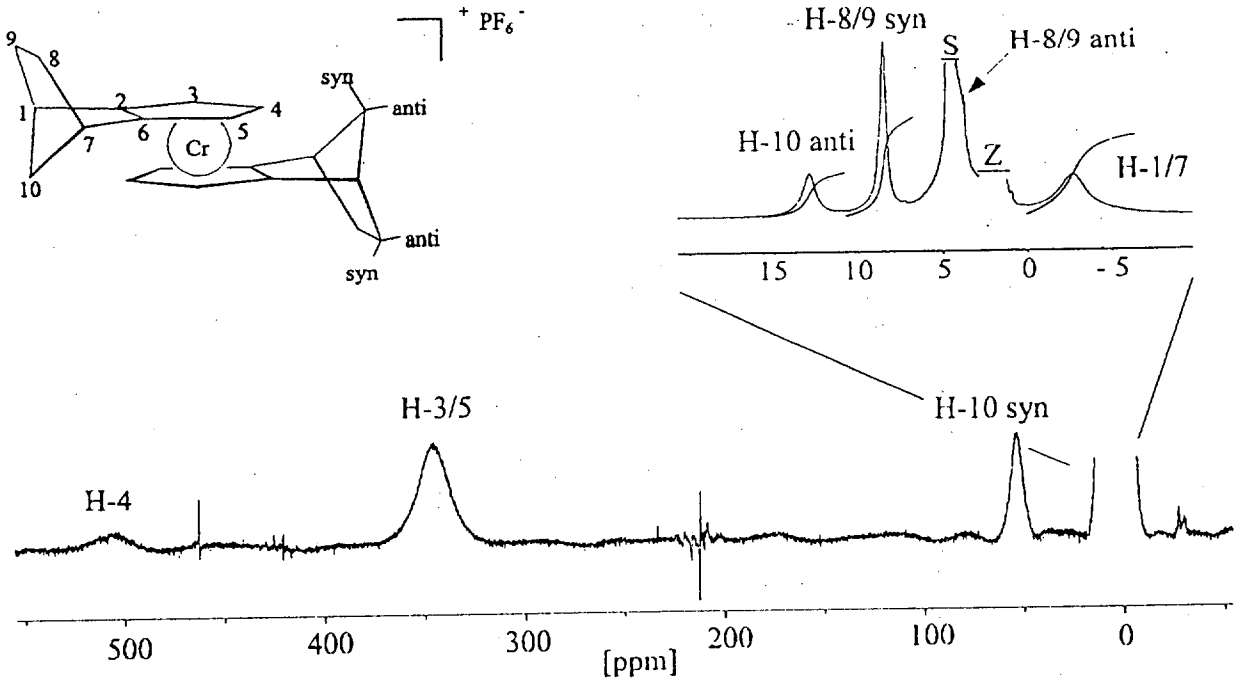

Figure S7. ^{1}H NMR spectrum of **5a**$^+PF_6^-$ in CD_3NO_2 at 297 K. S = solvent, Z = diamagnetic impurities.

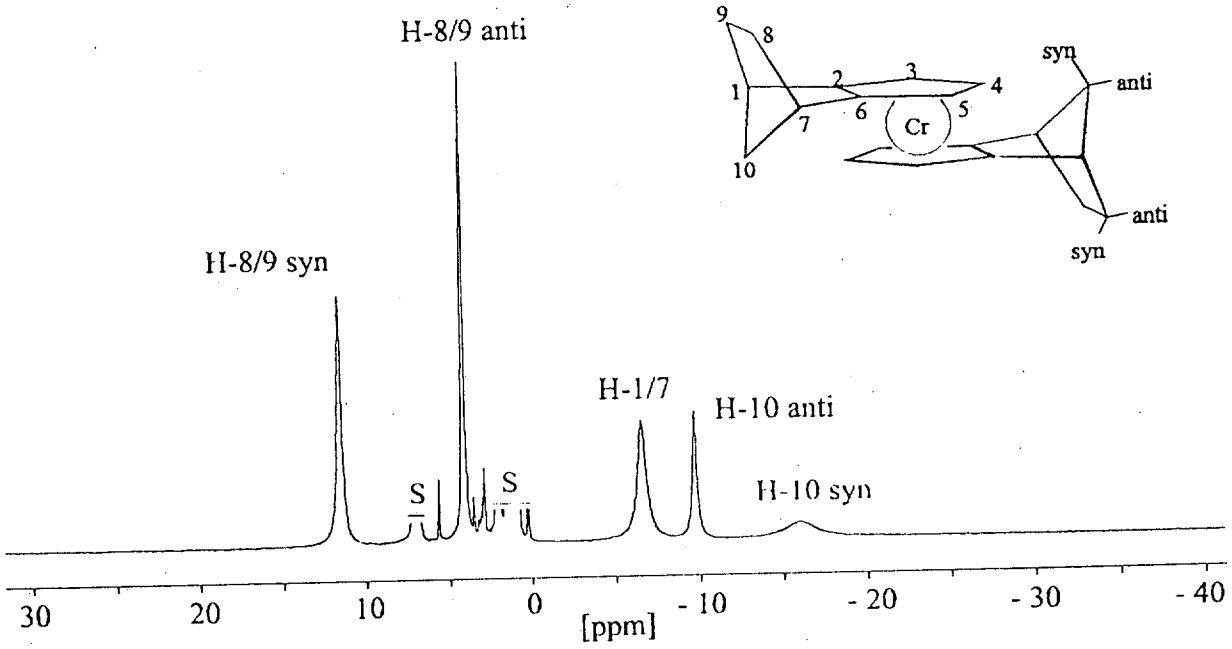

Figure S8. ^{1}H NMR spectrum of **5a** in toluene-d_8 at 305 K. S = solvent.

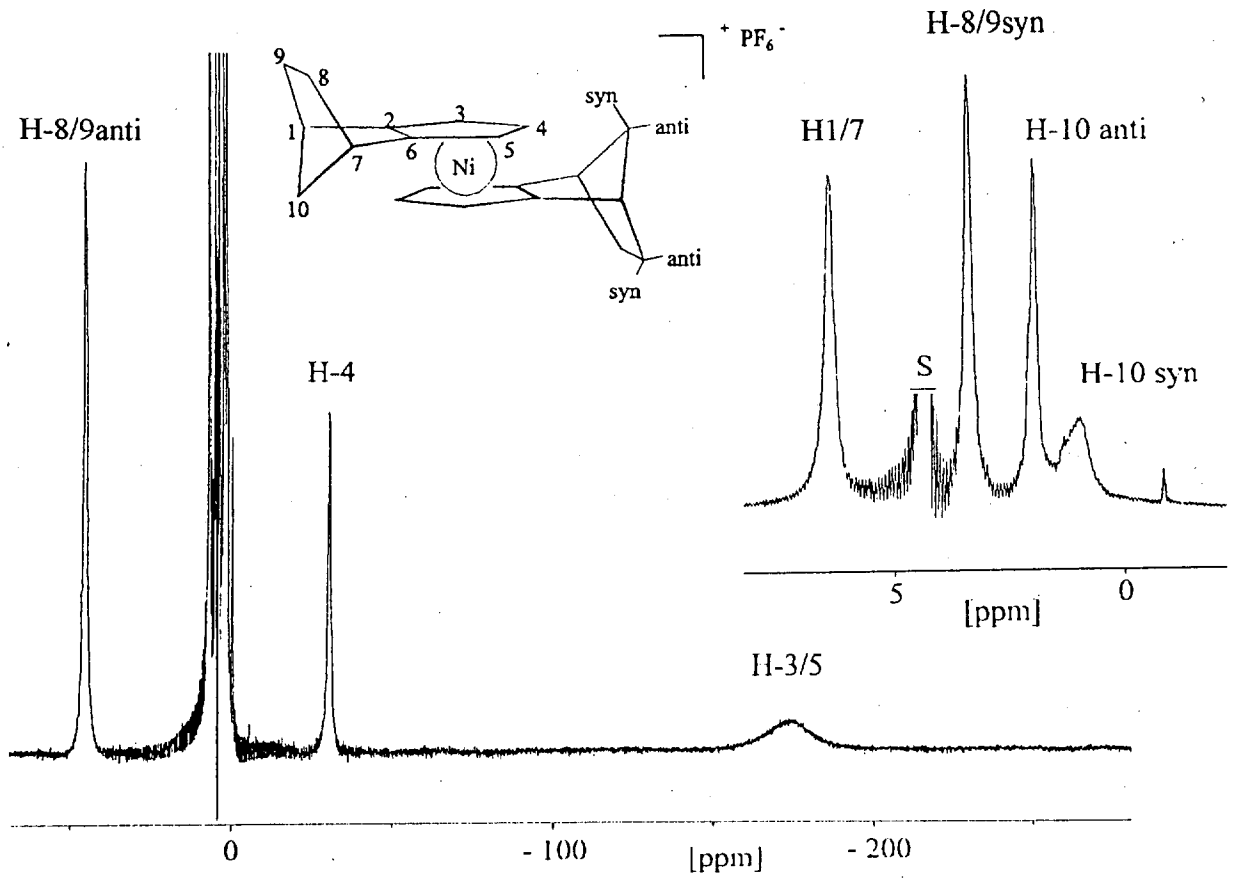

Figure S9. ^{1}H NMR spectrum of **7a**$^+$$PF_6^-$ in CD_3NO_2 at 305 K. S = solvent.

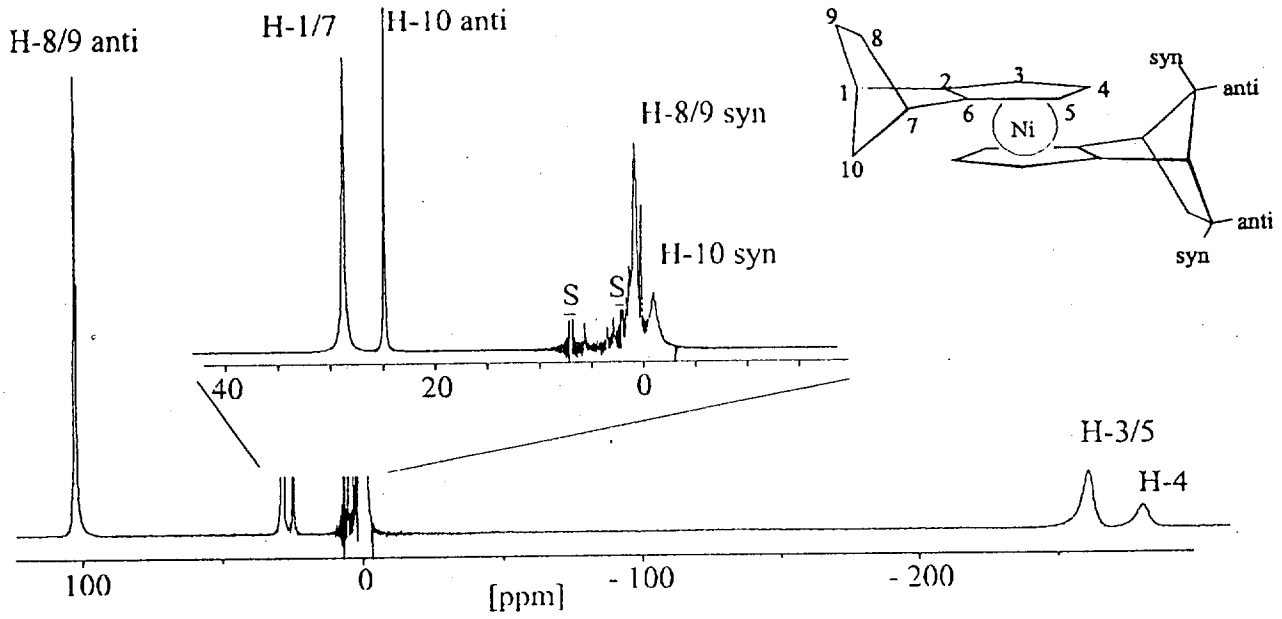

Figure S10. ^{1}H NMR spectrum of **7a** in toluene-d_8 at 298 K. S = solvent

Calculation of the Dipolar Signal Shifts

The calculations are based on the work of Kurland and McGarvey.[24] For a given spin multiplicity and temperature T the dipolar shift δ^{dip}_{T} depends on the g factors $g_{\parallel}$ and $g_{\perp}$ and on the geometric factor of the nucleus under study, $G(r, \theta) = (3\cos^2\theta - 1)/r^3$, where r is the length of metal-nucleus vector and θ is the angle between that vector and the magnetic axis which is assumed to coincide with the Cp-M-Cp axis. The geometric factors were taken from the positional parameters which were obtained as a by-product of the EHMO calculations and which are listed in Table S1. When more than one unpaired electron is present, δ^{dip} also depends on the zero-field splitting D. The latter term is included in the proportionality constant of the formula for the various cases:

3a$^+PF_6^-$ and **3b**$^+PF_6^-$:

$S = 1/2$, $g_{\parallel} = 3.9561$, $g_{\perp} = 2.0560$, $T = 305$ K

$$\delta^{dip}_{305} = 1.9446 \times 10^{-3} \quad G(r, \theta) \tag{S1}$$

7a$^+PF_6^-$:

$S = 1/2$, $g_{\parallel} = 1.768\text{-}1.878$[S1], $g_{\perp} = 1.865\text{-}2.024$[S1], $T = 305$ K;

within the g-factor limits one gets

$$\delta^{dip}_{305} = -1.0526 \times 10^{-4} \quad G(r, \theta) \text{ and} \tag{S2a}$$

$$\delta^{dip}_{305} = -6.5272 \times 10^{-5} \quad G(r, \theta) \tag{S2b}$$

(S1) Zoller, L.; Moser, E.; Ammeter, J.H. *J. Phys. Chem.* **1986**, *90*, 6632.

7a:

$S = 1$, $g_{\parallel} = 2.0023$[S2], $g_{\perp} = 2.11$[S2], $D = 33.6\ cm^{-1}$[S2],

$T = 305$ K and 379 K

$$\delta^{dip}_{305} = -3.507 \times 10^{-4} \qquad G(r, \theta) \qquad \text{(S3)}$$

$$\delta^{dip}_{379} = -2.587 \times 10^{-4} \qquad G(r, \theta) \qquad \text{(S4)}$$

5a:

$S = 1$, $g_{\parallel} = 2.33$[S3], $g_{\perp} = 2.77$[S3], $D = 15.1\ cm^{-1}$[S3], $T = 305$ K

$$\delta^{dip}_{305} = -9.191 \times 10^{-4} \qquad G(r, \theta) \qquad \text{(S5)}$$

5a$^{+}PF_6^{-}$:

$S = 3/2$, $g_{\parallel} = 1.911$, $g_{\perp} = 1.7985$, $D = 1.461\ cm^{-1}$, $T = 297$ and 305 K

$$\delta^{dip}_{279} = 3.387 \times 10^{-4} \qquad G(r, \theta) \qquad \text{(S6)}$$

$$\delta^{dip}_{305} = 3.304 \times 10^{-4} \qquad G(r, \theta) \qquad \text{(S7)}$$

4a:

$S = 3/2$, $g_{\parallel} = 1.9790$, $g_{\perp} = 1.8627$, $D = 2.7\ cm^{-1}$[S4], $T = 345$ and 365 K

$$\delta^{dip}_{345} = 2.979 \times 10^{-4} \qquad G(r, \theta) \qquad \text{(S8)}$$

$$\delta^{dip}_{365} = 2.835 \times 10^{-4} \qquad G(r, \theta) \qquad \text{(S9)}$$

(S2) Baltzer, P.; Furrer, A.; Hulliger, J.; Stebler, A. *Inorg. Chem.* **1988**, *27*, 1543.

(S3) Worst case asumed from the data given in Desai V.P.; König, E.; Kanellakopulos, B. *J. Chem. Phys.* **1983**, *78*, 6299. König E.; Schnakig, R.; Kremer, S.; Kanellakopulos, B.; Klenze, R. *Chem. Phys.* **1978**, *27*, 331.

(S4) Prins, R.; van Voorst, J.D.W. *Chem. Phys.* **1968**, *49*, 4665.

Besides G(r, θ) Table S1 contains the paramagnetic signal shifts $\delta^{para}{}_T$ at the experimental tempereature T (obtained after subtracting the signal shifts of the diamagnetic standards from the experimental signal shifts δ^{exp} of Table 2), and the dipolar signal shift $\delta^{dip}{}_T$ (obtained from eqs S1-S9). Substraction of $\delta^{dip}{}_T$ from $\delta^{para}{}_T$ and conversion to the standard temperature of 298 K according to the Curie law gave the contact shifts δ^{con} listed in Table 2).

Table S1 Relevant Data[a] for the Calculation of the Dipolar Signal Shifts

nucleus and position[b]	**4a**			**3a**$^+$ / **3b**$^+$, *exo-ligand*		
	δ^{para}_{T} [c]	$G(r,\theta)$	δ^{dip}_{T} [c]	δ^{para}_{305}	$G(r,\theta)$	δ^{dip}_{305}
H3/5	231.2	0.0134	3.8	22.6[d]	0.0034	6.7
H4	231.0	0.0131	3.7	24.1[d]	0.0056	10.9
H1/7	-1.8	-0.0041	-1.2	14.8	-0.0010	-1.9
H8/9-*syn*	26.7	0.0100	2.8	23.5	0.0123	23.9
H8/9-*anti*	1.4	0.0034	1.0	6.7	0.0005	5.8
H10-*syn*	8.1	-0.0041	-8.7	-63.9	-0.0392	-76.2
H10-*anti*	-0.4	-0.0305	-1.8	-17.5	-0.0066	-12.9
C2/6	-527.0	0.0971	28.9	84.0	0.0986	191.8
C3/5	-607.5	0.0940	28.0	232.8	0.1097	213.3
C4	-484.8	0.0988	29.5	56.8	0.1197	232.8
C1/7	516.7	0.0048	1.4	-10.8	0.0007	1.3
C8/9	-67.1	0.0086	2.6	-115.6	0.0088	17.2
C10	569.2	-0.0117	-3.5	5.4	-0.0148	-28.8

Table S1 continued

nucleus and position[b]	**3b**$^+$, *endo*-ligand			**5a**		
	δ^{para}_{305}	G(r,θ)	δ^{dip}_{305}	δ^{para}_{305}	G(r,θ)	δ^{dip}_{305}
H3/5	23-26[d]	0.0034	6.7	294.5	0.0115	-10.6
H4	23-26[d]	0.0056	10.9	399.1	0.0110	-10.1
H1/7	-14.0	-0.0010	-1.9	-9.4	-0.0052	4.8
H8/9-*syn*	-42.2	-0.0385	-74.8	10.5	0.0103	-9.5
H8/9-*anti*	19.1	-0.0111	-21.6	2.4	0.0033	-3.0
H10-*syn*	23.6	0.0134	26.0	-18.4	-0.0316	29.0
H10-*anti*	5.6	0.0001	0.2	-11.2	-0.0071	6.5
C2/6	25.2	0.0986	191.8	-474.4	0.1025	-94.2
C3/5	216.2	0.1097	213.3	-262.9	0.0989	-90.9
C4	18.5	0.1197	232.8	-585.8	0.1041	-95.7
C1/7	25.9	0.0007	1.3	384.7	0.0034	-3.1
C8/9	-191.4	0.0241	46.8	-181.7	0.0086	-7.9
C10	25.2	0.0065	12.6	105.8	-0.0135	12.4

Table S1 continued

nucleus and position[b]	5a+			7a		
	δ^{para}_{T} [e]	G(r, θ)	δ^{dip}_{T} [e]	δ^{para}_{T} [f]	G(r, θ)	δ^{dip}_{T} [f]
H3/5	334.5	0.0115	3.9	-264.5	0.0106	-3.7
H4	504.4	0.0114	3.9	-284.0	0.0100	-3.5
H1/7	-6.1	-0.0051	-1.7	26.0	-0.0057	2.0
H8/9-*syn*	2.8	0.0127	4.3	-0.2	0.0104	-3.7
H8/9-*anti*	6.5	0.0039	1.3	100.8	0.0033	-1.2
H10-*syn*	51.5	-0.0318	-10.8	-3.3	-0.0322	11.3
H10-*anti*	11.1	-0.0066	-2.2	23.5	-0.0073	2.6
C2/6	-414.6	0.1029	34.0	1075[g]	0.1044	-27.0
C3/5	-328.8	0.1008	33.3	1075[g]	0.1020	-26.4
C4	-451.7	0.1064	36.0	1075[g]	0.1060	-27.4
C1/7	414.3	0.0048	1.6	-366.5	0.0028	-1.0
C8/9	-418.8	0.0098	3.2	1372.7	0.0086	-3.0
C10	271.7	0.0114	3.8	508.3	-0.0142	5.0

Table S1 continued

nucleus and position[b]	**7a**$^+$		
	δ^{para}_{305}	$G(r,\theta)$	δ^{dip}_{305} [h]
H3/5	-179.8	0.0086	-0.8
H4	-36.4	0.0081	-0.7
H1/7	3.2	-0.0064	0.6
H8/9-*syn*	2.3	0.0131	-1.1
H8/9-*anti*	43.3	0.0039	-0.3
H10-*syn*	-1.3	-0.0330	2.9
H10-*anti*	0.2	-0.0072	0.6
C2/6	239.4	0.1079	-9.4
C3/5	477.2	0.1052	-9.1
C4	-161.2	0.1111	-9.7
C1/7	-115.7	0.0032	-0.3
C8/9	116.9	-0.0133	0.9
C10	17.5	0.0099	-1.2

[a] Shifts in ppm, $G(r,\theta)$ in $Å^{-3}$. [b] Numbering see Figure 5. [c] ^1H and ^{13}C NMR data at 365 and 345 K, respectively. [d] For **3b**$^+PF_6^-$ a broad feature between 27 and 30 ppm was detected. [e] ^1H and ^{13}C NMR data at 297 and 305 K, respectively. [f] ^1H and ^{13}C NMR data at 298 and 379 K, respectively. [g] Broad feature. [h] Calculated with a mean value of eqs S2a and S2b.